

# Space Weather®



## RESEARCH ARTICLE

10.1029/2022SW003381

### Key Points:

- The consequences of space weather on communication, navigation, surveillance, and cosmic radiation in aviation are explored
- The aviation economic costs caused by space weather are estimated based on the analysis of the air traffic management system
- The cost incurred from satellite-based navigation failure is the least due to the backup of the ground navigation system

### Supporting Information:

Supporting Information may be found in the online version of this article.

### Correspondence to:

J. Yang and Z. Liu,  
yangj36@sustech.edu.cn;  
lszzliu@polyu.edu.hk

### Citation:

Xue, D., Yang, J., Liu, Z., & Yu, S. (2023). Examining the economic costs of the 2003 Halloween storm effects on the North Hemisphere aviation using flight data in 2019. *Space Weather*, 21, e2022SW003381. <https://doi.org/10.1029/2022SW003381>

Received 8 DEC 2022

Accepted 16 FEB 2023

### Author Contributions:

**Formal analysis:** Dabin Xue

**Software:** Shiwei Yu




**Supervision:** Jian Yang, Zhizhao Liu

**Visualization:** Shiwei Yu

**Writing – original draft:** Dabin Xue

**Writing – review & editing:** Jian Yang, Zhizhao Liu

## Examining the Economic Costs of the 2003 Halloween Storm Effects on the North Hemisphere Aviation Using Flight Data in 2019

Dabin Xue<sup>1,2</sup> , Jian Yang<sup>2</sup> , Zhizhao Liu<sup>1</sup> , and Shiwei Yu<sup>1</sup> 

<sup>1</sup>Department of Land Surveying and Geo-Informatics, The Hong Kong Polytechnic University, Hong Kong, China,

<sup>2</sup>Department of Earth and Space Sciences, Southern University of Science and Technology, Shenzhen, China

**Abstract** Space weather can impede normal aviation operations through communication blackouts, GNSS-based navigation and surveillance failures, and elevated cosmic radiation, consequently resulting in necessary flight plan adjustments and considerable economic costs. Although space weather effects have been heavily emphasized, the literature on the economic effects on aviation is limited. In this study, we estimate the economic impacts from the perspective of air traffic management, assuming an extremely strong space weather event like the 2003 Halloween solar storm would occur in 2019 with a booming air transport industry in recent years. We find that (a) as the high-frequency communication blackouts may lead to polar flight rerouting and cancellations, possible daily economic costs could range from €0.21 million to €2.20 million per day; (b) during the satellite navigation failure period in the continental United States, as aircraft utilizes ground navigation aids as a backup, the increased flying time and disrupted descent approach operations may lead to additional cost of €2.43 million; (c) a surveillance failure can reduce airspace capacity and increase the workload of air traffic controllers, resulting in fatigue and perhaps risking flight safety; (d) to prevent massive cosmic radiation exposure, the economic costs of flight cancellations can be from €2.77 million to €48.97 million, depending on the cosmic radiation dose limits for a given plan. Our study indicates that severe space weather events may briefly disrupt normal aviation operations and cause substantial economic losses if future aviation equipment and technology are fragile to its effects.

**Plain Language Summary** Space weather events have the potential to have a significant economic impact on many vital national infrastructure systems, including electricity grids, the oil and gas industry, and Global Navigation Satellite Systems (GNSS). Particularly, space weather can impair normal aviation operations from high-frequency communication blackouts, satellite navigation failure, GNSS-based surveillance failure, and enhanced aviation radiation exposure. Consequently, air traffic management methods are required, and the economic effects of space weather on aviation are inevitable. Due to the lack of actual flight operation data during past space weather events, it is still unclear what the economic losses will be. Therefore, this study tries to estimate the economic costs based on the assumption that a space weather event like the Halloween solar storm of 2003 would occur in 2019. We can conclude that the cost caused by massive cosmic radiation dose is the highest due to flight cancellations. In contrast, the cost caused by satellite navigation failure is the least due to the backup of ground navigation systems. We believe this study can serve as a baseline for future space weather economic implications.

## 1. Introduction

The study of space weather is increasingly important as space weather can affect a vast array of technologies and activities in space and on Earth, including Critical National Infrastructure (CNI) systems such as power grids (Watari, 2015), the oil and gas industry (Viljanen et al., 2006), communications (Kelly et al., 2014), ground transportation (Eroshenko et al., 2010), satellite infrastructure (Loto'aniu et al., 2015), and Global Navigation Satellite Systems (GNSS) (Humphreys et al., 2010). The Sun is the ultimate cause of space weather, which occasionally erupts solar flares (Svestka, 2012), Coronal Mass Ejections (CME) (Webb & Howard, 2012), and Solar Energetic Particles (SEP) (Ryan et al., 2000). The interaction between CME and the Earth's magnetic field can produce major geomagnetic storms (Gonzalez et al., 1999). Radio blackouts, solar radiation storms, and geomagnetic storms are recognized as the three fundamental types of space weather (Eastwood et al., 2017). Due to the

© 2023. The Authors.

This is an open access article under the terms of the [Creative Commons Attribution License](#), which permits use, distribution and reproduction in any medium, provided the original work is properly cited.

**Table 1**  
*Estimate of the Economic Costs of Space Weather Events*

Space weather events	Impact types	Geographic footprints	Duration	Costs	References
1859 Carrington-like storm	Lost revenue	—	—	\$44 billion	Odenwald et al. (2006)
	GEO satellite replacements	—	—	\$24 billion	
1859 Carrington-like storm	Power outages	The U.S.	16 days to 1–2 years	\$0.6–2.6 trillion	Maynard et al. (2013)
1859 Carrington-like storm	Critical infrastructure failure	The U.K.	First day	£2.9–15.9 billion	E. J. Oughton et al. (2019)
1989 Quebec-like storm	Power outages	Quebec	9 hr	\$13.2 million	Bolduc (2002)
1989 Quebec-like event	Supply chain disruptions	The global	One year	\$2.4–3.4 trillion	Schulte in den Bäumen et al. (2014)
S1	Power failure	The U.S.	Daily	\$220 billion	E. Oughton et al. (2016)
S2				\$700 billion	
X1				\$1.2 trillion	
S1	Electricity transmission	55° ± 2.75°N in the U.S.	Daily	\$6.2 billion	E. J. Oughton et al. (2017)
S2	infrastructure failure	50° ± 2.75°N in the U.S.		\$37.7 billion	
S3		45° ± 2.75°N in the U.S.		\$16.5 billion	
S4		50° ± 7.75°N in the U.S.		\$41.5 billion	
1989 Quebec-like storm	Power outage	Western Europe	24 hr	€55.5 billion	Eastwood et al. (2018)
2003 Halloween-like storm				€668 million	

*Note.* The definitions of S1–S4 and X1 can refer to related references.

complexity and high interconnectedness of the underlying physical factors, all these three phenomena can occur within a single space weather event with various temporal and spatial footprints and severity levels.

The development and enhancement of communications, navigation, and surveillance technologies are essential in the modernization of aviation (Schnell et al., 2014). Thus, the aviation industry is susceptible to solar events, which may affect High Frequency (HF) communications, cosmic radiation, and GNSS-based navigation and surveillance. To reduce the detrimental effects on aviation, space weather service is implemented by the joint operation of three global space weather centers, that is, Pan-European Consortium for Aviation Space weather User Services (PECASUS, which consists of 10 International Civil Aviation Organization (ICAO) members including Finland, Belgium, the United Kingdom, Austria, Germany, Italy, Netherlands, Poland, Cyprus, and South Africa), NOAA Space Weather Prediction Center (SWPC), and the consortium of Australia, Canada, France, and Japan (ACFJ) (Kauristie et al., 2021). These three space weather centers have been operational since November 2019 and provide the most up-to-date space weather alerts from the perspectives of HF communications, GNSS, and high solar radiation, which can be obtained via <http://www.bom.gov.au/aviation/space-weather-advisories/>. In addition, the Sino-Russian space weather monitoring center has begun to provide services for global aviation operators since 16 November 2021 (Li, 2021).

In the modern 21st century, a better understanding of the social and economic effects of space weather is a crucial but formidable problem. The economic costs of specific space weather events are summarized in Table 1 based on several assumptions, simplifications, extrapolations, and inferences. It indicates that the potential costs of historical moderate storms are in the millions of dollars, whereas the potential costs of theoretical extreme storms are in the billions to trillions of dollars.

Although the probability of recurrence of a severe space weather event is low, it is indeed likely to recur from a statistical point of view. To date, the economic costs due to space weather effects on aviation are still not clear, which is because of the lack of flight data and theoretical models. Therefore, to fill this research gap, we simulated a scenario using a historical space weather event and the actual flight data of 7 April 2019 (UT) from the Opensky to estimate the economic costs of space weather to aviation due to communication blackout, GNSS navigation failure, surveillance failure, and massive aviation radiation exposure from the standpoint of air traffic management. With the upcoming sunspot maximum, solar activity is expected to increase significantly in the following several years. We believe that this study can provide an approach for the aviation industry to evaluate and pre-calculate the space weather impacts for the future.

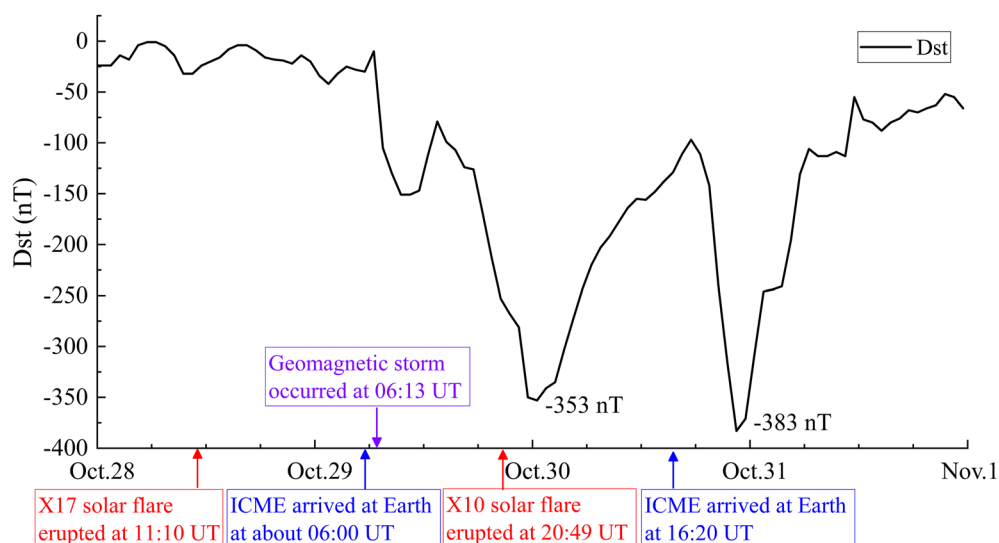


**Figure 1.** Space weather events and Dst during 28–31 October 2003 (Sparks et al., 2022).

The space weather event selected in this study is the Halloween storm, which occurred from mid-October to early November 2003 and peaked around 28–29 October 2003. Figure 1 shows the Dst index during 28–31 October 2003, which results from a series of solar flare eruptions, interplanetary coronal mass ejections (ICME), and a two-dip super geomagnetic storm (Gopalswamy et al., 2005). According to National Oceanic and Atmospheric Administration (NOAA) (NOAA, 2004), the impacts on aviation are summarized from the perspectives of communication, navigation, and cosmic radiation.

1. From 19 October 2003–5 November 2003, aviation radio communication disruption occurred every day, posing a threat to regular flight operations. Following an X1.1 (R3 [Strong]) solar flare during 16:29–17:04 UT on 19 October 2003, HF service was impaired for more than 2 hr, causing three polar trips (New York–Hong Kong) rerouting to more favorable datalink and Satellite Communication (SATCOM) routes, which resulted in additional consumption of 26,600 pounds of fuel and the reduction of over 16,500 pounds of cargo. In addition, additional staff was required to handle air traffic due to poor communications on 30 October 2003.
2. The Wide Area Augmentation System (WAAS) was severely degraded, prohibiting aircraft from utilizing WAAS for precise approaches. Localizer Performance with Vertical Guidance (LPV) service was interrupted for 15 hr on 29 October 2003 and 11 hr on 30 October 2003 across the Continental United States (CONUS).
3. The Federal Aviation Administration (FAA) released solar radiation levels on 28–29 October, indicating that flights going north or south of 35° latitude were susceptible to high radiation doses. To control aviation radiation exposure, some polar flights were rerouted to non-polar routes, despite necessitating fuel stops in Japan. Besides, flights between the U.S. and Europe also lowered flight altitudes.

## 2. Communication Blackout

The ICAO requires that aircraft maintain continuous and effective communications throughout their entire flight routes (ICAO, 2008). Aircraft generally use the Very High Frequency (VHF, 30–300 MHz) to communicate with ground stations. To be specific, the Aircraft Communications Addressing and Reporting System (ACARS, 131.550 MHz) based on geostationary satellites is used to connect with airlines, while the Controller Pilot Data Link Communication (CPDLC, 118.000–136.975 MHz) is used to achieve the communications between pilots and Air Traffic Control Officers (ATCOs). VHF communication via satellite is not available to the north of 82°N or south of 82°S, because SATCOM is not feasible at such high latitudes (Sauer & Wilkinson, 2008). Therefore HF (3–30 MHz) radio is the only means of contact when airplanes fly over the pole regions. For example, Delta airline requires that all aircraft utilize HF radio as the primary mode of communication when flying in the area where the latitudes are higher than the latitude of waypoint ORVIT (79.00°N, 168.97°W) (Delta, 2010).

During Solar Proton Events, solar protons strike the ionosphere, leading to a decrease in the reflection height and an increase in the HF absorption termed Polar Cap Absorption (PCA) (Cameron et al., 2022; Neal et al., 2013).

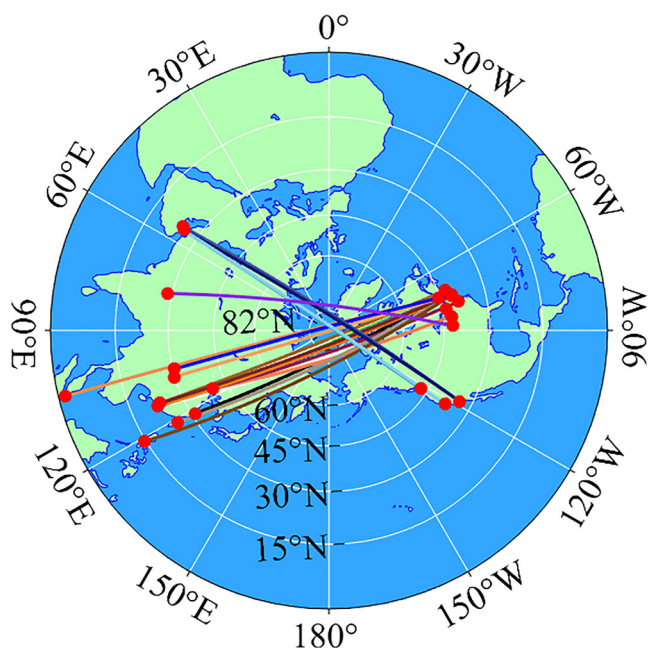


**Figure 2.** Schematic of the great circle routes for polar flights in different color lines. The red solid circles denote airports.

PCA can disrupt HF communications in the polar regions, and therefore aircraft in the polar regions cannot communicate with HF radio. On the sunlit side of the Earth, solar flares can disable HF communications for a few hours, while solar radiation storms can affect HF radios for several days (Rutledge & Desbios, 2018). Consequently, polar flights are requested to reroute to latitudes below 82° for keeping the line of sight with the satellites since polar routes are more susceptible to the effects of space weather on communications (National Research Council, 2008).

In response to the communication blackout, airborne flights would reroute to the destination airport or land at an alternative airport, but those on the ground would probably not be allowed to take off as scheduled (Cannon et al., 2013). Although airlines can reroute flights with the assistance of Air Navigation Service Providers (ANSPs) to avoid the PCA region, it has several drawbacks from the viewpoint of air traffic management. First, rerouting always causes increased fuel consumption, aircraft emissions, and additional wear and tear on aircraft, which can disturb normal aircrew schedules and contradict the green aviation concept. Second, the temporary or unauthorized flight routes will infringe on the sovereignty of the airspace. Third, communication blackouts are often accompanied by increased cosmic radiation exposure weather, which can be hazardous to the health of aircrews and passengers. Due to the aforementioned three reasons, airlines would like to cancel polar flights justifiably, notwithstanding the associated cancellation costs (Yamashiki et al., 2020).

We assume that a space weather event as strong as the Halloween storm will cause the cancellation of polar flights for one entire day due to communication blackouts. The cancellation costs include passenger care and compensation costs, loss of revenue, interlining costs, passenger opportunity costs, crew and catering costs, luggage delivery costs, operational savings, ground handling costs, etc. (EUROCONTROL, 2020). The historical flight data on 7 April 2019 is adopted in this simulation, which includes a total of 48 polar flights including 38 flights of 400 seats, 3 flights of 250 seats, and 7 flights of 180 seats. Polar flight routes are now common for connecting Asia and North America. As we did not get the actual polar flight trajectories, we use the great circle routes to represent polar routes (see Figure 2). Please note that we do not consider polar flights via the Antarctic because no airline has scheduled such a route. Space weather is classified as extraordinary circumstances, so airlines are not required to compensate passengers. According to Table 2, the projected daily cost of polar flight cancellations is about €2.20 million per day (82,670 + 119,970 + 1,992,720). If all polar aircraft were to be rerouted, the total increased fuel cost would be €0.21 million ( $26,600 \times 0.4536 \div 3 \times 48 \times 1.139$ , referring to point (1) in Section 1) based on the additional fuel consumption caused by flight rerouting (NOAA, 2004) and the price of €1139 per ton of fuel (IATA, 2022).

### 3. GNSS-Based Navigation Failure

The operation of GNSS is based on the trilateration mathematical principle. The accuracy of GNSS positioning and navigation depends on many factors, such as satellite clock error (Guo & Geng, 2018), satellite orbit error

**Table 2**  
EUROCONTROL Recommended Flight Cancellation Costs (EUROCONTROL, 2020)

Cancellation cost (€)	Narrow-body aircraft			Wide-body aircraft	
Number of Seats	50	120	180	250	400
Cancellation costs (€)	6,540	16,040	24,900	82,730	120,830
Within passenger care and compensation (€)	3,280	8,020	13,090	42,740	68,390
Cancellation costs excluding passenger care and compensation (€)	3,260	8,020	11,810	39,990	52,440
The number of daily polar flights	0	0	7	3	38
The daily cost of polar flight cancellations (€)	0	0	82,670	119,970	1,992,720

(Zhang et al., 2019), ionospheric delay (Yu & Liu, 2021), tropospheric delay (Chen & Liu, 2015), receiver noise (Kim et al., 2019), and multipath effect (Sun et al., 2019). The main observation in GNSS positioning is the pseudorange measurements  $\tilde{\rho}$  from the receiver ( $r$ ) to the satellite ( $s$ ) (Langley et al., 2017):

$$\tilde{\rho} = \rho + c(\Delta t_r - \Delta t^s) + \Delta \rho_I + \Delta \rho_T + \varepsilon \quad (1)$$

where  $\rho$  is the geometric distance between the GNSS satellite and GNSS receiver;  $c$  is the speed of light in vacuum;  $\Delta t_r$  is the offset of the receiver clock to GNSS time at signal reception time;  $\Delta t^s$  is the offset of the satellite clock to GNSS time at signal emission time;  $\Delta \rho_I$  is the ionospheric delay correction;  $\Delta \rho_T$  is the tropospheric delay correction;  $\varepsilon$  is the measurement error of the observation. Among these errors, the ionospheric delay is the largest error source ranging from a few meters to tens of meters or even hundreds of meters (Z. Yang et al., 2020). When GNSS signals propagate in the ionosphere, the propagation is delayed when compared with that in the vacuum. In addition, spatial gradients in the refractive index cause a propagation curve. Both effects can lead to increased vulnerability and degraded accuracy in satellite-based positioning and navigation. The ionospheric delay error is proportional to the ionospheric total electron contents (TEC) along the propagation path and inversely proportional to the square of the radio frequency  $f$ , which can be expressed as follows:

$$\Delta \rho_I = -\kappa \frac{\text{TEC}}{f^2} \quad (2)$$

where  $\kappa \approx 40.3 \text{ m}^3 \text{ s}^{-2}$ ,  $f$  is the radio frequency (in Hz), and TEC is the total number of electrons integrated between two points along a tube of a one-m square cross section. The unit of TEC is called TEC units (TECU) ( $1 \text{ TECU} = 10^{16} \text{ electron/m}^2$ ).

The Movie S2 shows the temporal and spatial distribution of TEC during 27–31 October 2003. Under normal circumstances after sunset, the recombination of free electrons and positive ions lowers the background ionization. However, the plasma density structure displaying substantial TEC gradients remained for several hours into the night after sunset. Ionospheric irregularity occurring in the morning of 31 October had a TEC level exceeding 60 TECU. Previous studies showed that CONUS had been affected severely by this space weather (Doherty et al., 2004), so in this study, we focus on the top 50 busiest airports in CONUS and select the nearby Continuously Operating Reference Stations (CORS), which are the nearby GNSS stations to related airports, are selected as the source to obtain GNSS data for analysis. Figure 3 shows the positioning errors of nine representative GNSS stations along with the Dst index. It is required that positioning errors of GPS standard positioning service for aviation operations not exceed 17 m horizontally and 37 m vertically (ICAO, 2018). The satellite navigation failure durations can be calculated based on Figure 3, and the detailed results are accordingly shown in Table 3. Due to data restrictions, we characterize GNSS station positioning failure only in terms of accuracy rather than integrity, continuity, or availability. The affected airports are denoted “Y” in Figure 4 based on the Single Point Positioning (SPP) method.

Traditionally, ground-based navigational aids, such as Very High-Frequency Omnidirectional Range (VOR), Distance Measuring Equipment (DME), and Non-Directional Beacon (NDB), are employed as a backup in the absence of GNSS-based navigation. When the GNSS-based Area Navigation (RNAV) is in an outage, traditional ground-based navigational methods are used. Consequently, the flight distance and time will increase since ground navigational routes are typically curved. Taking the Jackson Hole airport as an example, the flight route based on ground navigation is 14 miles and 3 min longer than the satellite navigation router (Enge et al., 2015). According to the Base of Aircraft Data (BADA) (EUROCONTROL, 2022), it would take an average of 105 kg of fuel for each aircraft during a three-minute approaching flight. Besides, GNSS navigation failure will hinder the Continuous Descent Approach (CDA) and the step-down approach has to be adopted for descending. Studies showed that this would increase fuel consumption by 147 kg per flight during the descent phase at the Hartsfield-Jackson Atlanta International Airport (Cao et al., 2014). The schematic of RNAV and CDA is illustrated in Figure 5.

The induced economic costs are assessed from the perspectives of several stakeholders, including airlines, passengers, and the environment. The fuel cost is the top expenditure of airlines (Wen et al., 2022), with fuel price  $C_F = \text{€}1139/\text{ton}$  (IATA, 2022). Passengers pay more attention to the boarding time. For a typical B757 configuration with an occupancy of 80%, the unit time cost for all onboard passengers  $C_T$  is equal to  $\text{€}93/\text{min}$  (Xue, Yang, & Liu, 2022). Additionally, the environmental impact such as the greenhouse effect  $\text{CO}_2$ , has a social cost  $C_{\text{CO}_2} = \text{€}417/\text{ton}$  (Ricke et al., 2018). On average, aircraft burning 1 kg of fuel will emit 3.15 kg  $\text{CO}_2$  during flight (Xue, Liu,



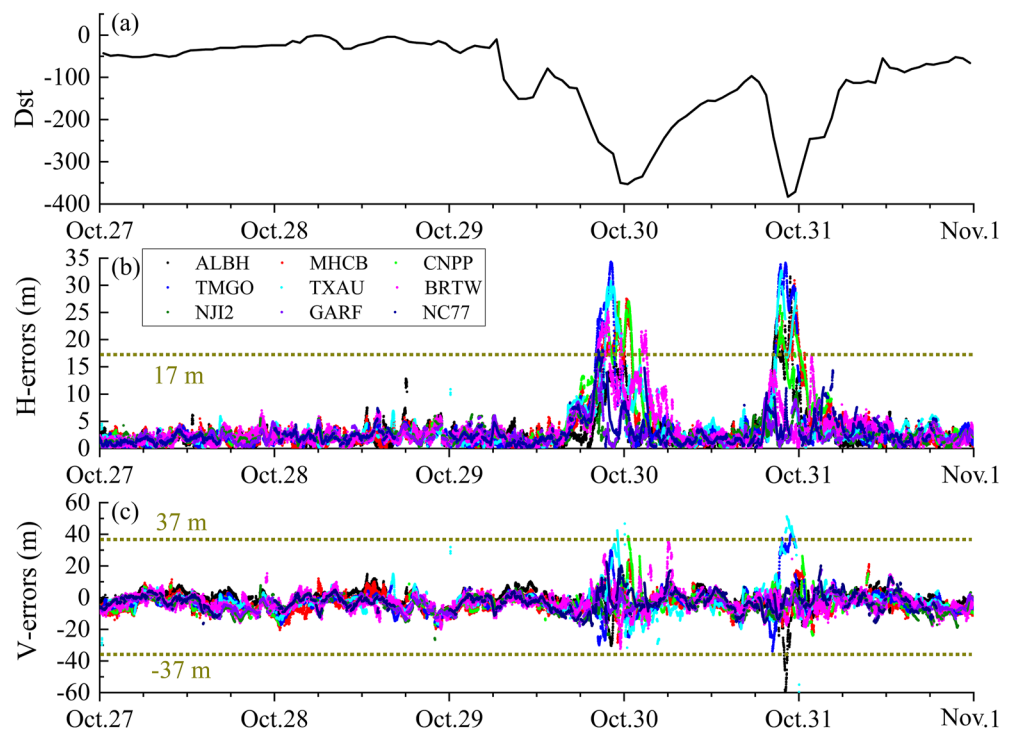


**Figure 3.** (a) The values of Dst index during 28–31 October 2003, (b) Global Navigation Satellite Systems (GNSS) Standard Positioning Service horizontal errors at nine Continuously Operating Reference Stations (CORS) stations during 27–31 October 2003; (c) GNSS Standard Positioning Service vertical errors at nine CORS stations during 27–31 October 2003.

et al., 2021). Therefore, the total induced cost per aircraft is  $\Delta C = C_F \cdot \Delta F + C_T \cdot \Delta T + C_{CO_2} \cdot \Delta CO_2 = \text{€}897$ , with fuel cost (€287), time cost (€279), and environmental cost (€331). We can calculate that there were totally 17,922 flights arriving at these top 50 busiest airports using the flight data on 7 April 2019. Assuming the daily number of flights during the space weather event 28–31 October 2003 was the same as the one on 7 April 2019, we can calculate that 2,705 flights would be affected during the whole space weather events based on the duration data of GNSS navigation failure in Table 3 and the total economic cost was estimated as €2.43 million.

#### 4. Surveillance Failure

Space weather events can degrade GNSS performance and consequently cause failure in Automatic Dependent Surveillance-Broadcast (ADS-B), which is mainly based on GNSS. Figure 6a shows that the positions of aircraft are determined by GNSS (Xue, Hsu, et al., 2021). The onboard ADS-B out system periodically broadcasts ADS-B messages at the frequency of 1,090 MHz, which can be received by ground ADS-B receivers and other aircraft equipped with ADS-B In-system (Jheng et al., 2020). These ADS-B signals are then transferred to the air traffic control center. After signal integration, the flight situations are displayed on the screen for air traffic management, as shown in Figure 6b. During the GNSS navigation failure period, ADS-B-based surveillance will be disabled. The radar system, as the alternate surveillance technique, will be used. Space weather events can also cause the failure of radar-based surveillance despite the low possibility. For example, Marqué et al. (2018) reported that on 4 November 2015, an exceptionally strong solar burst at radio frequency around 1 GHz occurred, causing strong radar disturbance of air traffic control in Sweden and some other European countries, when the radar antennas pointing at the Sun at that time.

When both radar and ADS-B are unavailable, procedure control will be used as a backup system, which uses an even higher aircraft separation standard, resulting in even smaller airspace capacity and more workload for air traffic controllers (ICAO, 2016). An increased workload on air traffic controllers during a particular work period may pose threats to flight safety. Air traffic controllers are directly responsible for the safe operation of air traffic. Their tasks consist of traffic monitoring, conflict resolution, flight vectoring, and communication with pilots and

**Table 3**  
*Duration of Global Navigation Satellite Systems (GNSS) Positioning Failure at GNSS Stations Nearby Airports*

ICAO code	City	Nearby CORS station	Lat (°N)	Lon (°W)	Distances to airports (km)	Start and end time of CORS station positioning failure DDHHMM–DDHHMM (duration in minutes)
KPDX	Portland	ALBH	48.39	123.49	108	292237–300007 (90 min) 302032–302307 (155 min)
KSEA	Seattle	ALBH	48.39	123.49	137	292237–300007 (90 min) 302032–302307 (155 min)
KSFO	San Francisco	OHLN	38.01	122.27	44	292056–300104 (248 min) 302048–310005 (197 min)
KOAK	Oakland	OHLN	38.01	122.27	33	292056–300104 (248 min) 302048–310005 (197 min)
KSJC	San Jose	MHCB	37.34	121.64	25	292054–300104 (250 min) 302050–310008 (198 min)
KSMF	Sacramento	SUTB	39.21	121.82	60	292059–300058 (239 min) 302040–302359 (199 min)
KLAX	Los Angeles	TORP	33.80	118.33	18	292045–300112 (267 min) 302054–310025 (211 min)
KSNA	Santa Ana	CNPP	33.86	117.61	31	292043–300109 (266 min) 302052–310015 (203 min)
KSAN	San Diego	BILL	33.58	117.06	95	292045–300040 (235 min) 302053–310015 (202 min)
KLAS	Las Vegas	BKAP	35.29	116.08	122	292046–300049 (243 min) 302052–310043 (231 min)
KPHX	Phoenix	AZGB	33.40	110.77	115	292020–300044 (264 min) 302051–310107 (256 min)
KSLC	Salt Lake City	TMGO	40.13	105.23	14	292008–292241 (153 min) 302045–302348 (183 min)
KDEN	Denver	TMGO	40.13	105.23	57	292008–292241 (153 min) 302045–302348 (183 min)
KSAT	San Antonio	TXAN	29.49	98.58	11	292124–292349 (145 min) 302051–302345 (174 min)
KAUS	Austin	TXAU	30.31	97.76	15	292120–292344 (144 min) 302054–302340 (166 min)
KDEW	Dallas	TXAU	30.31	97.76	296	292120–292344 (144 min) 302054–302340 (166 min)
KIAH	Houston	TXAU	30.31	97.76	20	292120–292344 (144 min) 302054–302340 (166 min)
KHOU	Houston	TXAU	30.31	97.76	17	292120–292344 (144 min) 302054–302340 (166 min)
KMSY	New Orleans	TXAU	30.31	97.76	61	292120–292344 (144 min) 302054–302340 (166 min)
KTPA	Tampa	BKVL	28.47	82.45	56	292021–292200 (99 min) 300219–300304 (45 min)

**Table 3**  
*Continued*

ICAO code	City	Nearby CORS station	Lat (°N)	Lon (°W)	Distances to airports (km)	Start and end time of CORS station positioning failure DDHHMM–DDHHMM (duration in minutes)
KRSW	Fort Myers	NAPL	26.15	81.78	43	292024–292208 (104 min) 300207–300332 (85 min) 300600–300612 (12 min) 302119–302131 (12 min)
KJAX	Jacksonville	PLTK	29.66	81.69	93	292019–292155 (96 min) 292337–292346 (9 min) 300159–300303 (64 min) 310155–310204 (9 min)
KMCO	Orlando	BRTW	27.95	81.78	70	292020–292201 (101 min) 292330–292341 (11 min) 300221–300307 (46 min)
KMIA	Miami	MTNT	25.87	80.91	63	292024–292207 (103 min)
KFLL	Miami	MTNT	25.87	80.91	79	292024–292207 (103 min)
KPBI	Palm Beach	OKCB	27.27	80.86	99	292021–292159 (98 min) 300224–300301 (37 min)

other traffic controllers. A sudden increase in workload may result in low efficiency and elevated fatigue for air traffic controllers. The possibility of human errors may increase accordingly. The effect of space weather on the working efficiency of air traffic controllers cannot be easily quantified. However, it cannot be simply ignored as the consequence of any occurrence of such a human-induced accident is serious.

## 5. Excessive Cosmic Radiation

Originating from the Sun and distant galaxies, cosmic radiation is composed of high-energy protons and atomic nuclei that travel through space at almost the speed of light. Excessive cosmic radiation exposure can cause various diseases and biological effects such as cancer, central nervous system damage, and DNA damage (NASA, 2017). The cosmic radiation intensity is dependent on altitude, geomagnetic latitude, and solar activity (Z.-Y. Yang & Sheu, 2020). The shielding effect of Earth's atmosphere and magnetic field against cosmic radi-

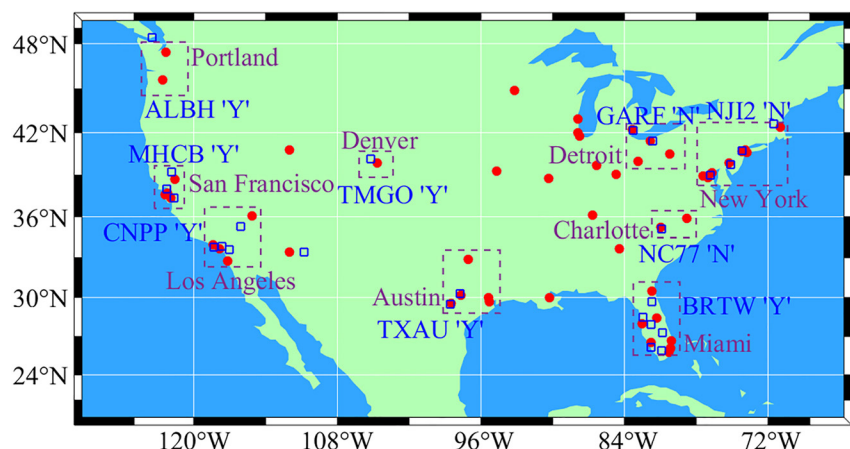


**Figure 4.** The location of the top 50 busiest airports (red circles) in the Continental United States and Global Navigation Satellite Systems (GNSS) stations (blue squares) nearby the airports. It should be noted that GNSS stations are not shown for every airport due to the unavailability of GNSS data nearby some airports. The areas showing GNSS positioning failure are labeled with “Y.”



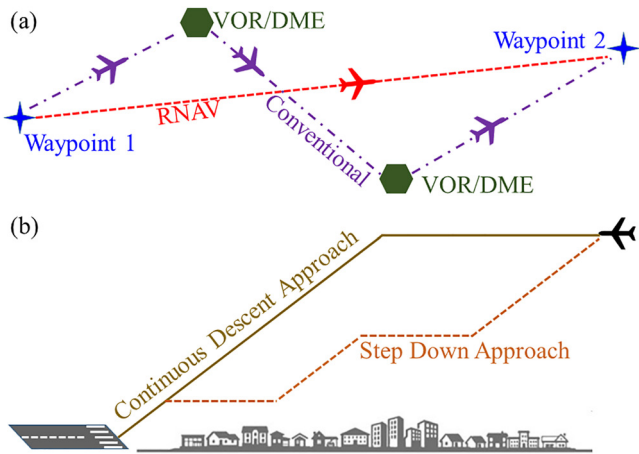


**Figure 5.** (a) The comparison between RNAV and conventional flight routes. Aircraft can fly directly from one waypoint to another waypoint based on satellite navigation. Without satellite navigation, aircraft are required to fly along the ground navigation aids; (b) With satellite navigation aid, aircraft can achieve the Continuous Descent Approach from cruise altitude to the runway in a smooth glide trajectory using low power, reducing fuel consumption and noise pollution. During satellite navigation failure, the step-down approach has to be used and fuel consumption is increased.

ation is stronger at the equator at lower altitudes and weaker at the poles at higher altitudes. Consequently, terrestrial inhabitants are largely insulated from the biological impacts of cosmic radiation (Tuo et al., 2012). The FAA regards aircrews as occupational radiation workers because aircrews always absorb a significant amount of cosmic radiation when flying at high altitudes with inadequate atmospheric protection (Bagshaw, 2008). Therefore, airline dispatchers are obligated to account for the cumulative cosmic radiation of flight crews while making flight plans. The International Commission on Radiological Protection (ICRP), FAA, and the European Union recommend an effective cosmic radiation dose limit of 20 mSv per year averaged over 5 years (a total of 100 mSv within 5 years) for aircrews and 1 mSv/year for the general public (ICRP, 2016). For pregnant radiation workers, the ICRP recommends a dose limit of 1 mSv throughout the whole pregnancy (ICRP, 2016). The National Council on Radiation Protection and Measurements also recommends a monthly radiation limit of 0.5 mSv during pregnancy (NCRP, 2013). Figure 7 shows the cosmic radiation rates at the altitude of 11 km from 27 October 2003–31 October 2003, calculated using the Nowcast of Aerospace Ionizing Radiation System (NAIRAS) (Mertens et al., 2013). Due to the lack of data on cosmic radiation rates in the Southern Hemisphere, we only consider flight situations in the Northern Hemisphere. As we did not have flight data during the 2003 Halloween storm, we assumed that the flight data of 7 April 2019, for which we had the flight data, were the same as those in the 2003 Halloween storm. Therefore, the flight data on 7 April 2019 (UT) were adopted. There were 45,822 flights in the Northern

Hemisphere on that day, and the recommended cancellation cost for each aircraft type is known according to (EUROCONTROL, 2020) (also see Table 2). We estimated the aviation radiation exposure of each flight during 27–30 October 2003.

The cosmic radiation rate at a given longitude  $x$  and latitude  $y$  at time  $t$  is denoted by  $r_{xyt}$  (in the unit of  $\mu\text{Sv}/\text{min}$ ), which is obtained from the NAIRAS. For simplicity, the Great circle routes are assumed to be the real flight routes. Because the first and last 30 min of the flight time are used for climbing and descending, we only consider the cruising period from  $T_s = T_d + 30$  to  $T_e = T_l - 30$  as the total exposure time of cosmic radiation.  $T_d$  and  $T_l$ , both in the unit of minutes, are the departure time at the origin airport and the landing time at the arrival airport, respectively. The total aviation cosmic radiation  $R_i$  of a certain flight  $i$  is given as

$$R_i = \int_{T_s}^{T_e} r_{xyt} dt \quad (3)$$

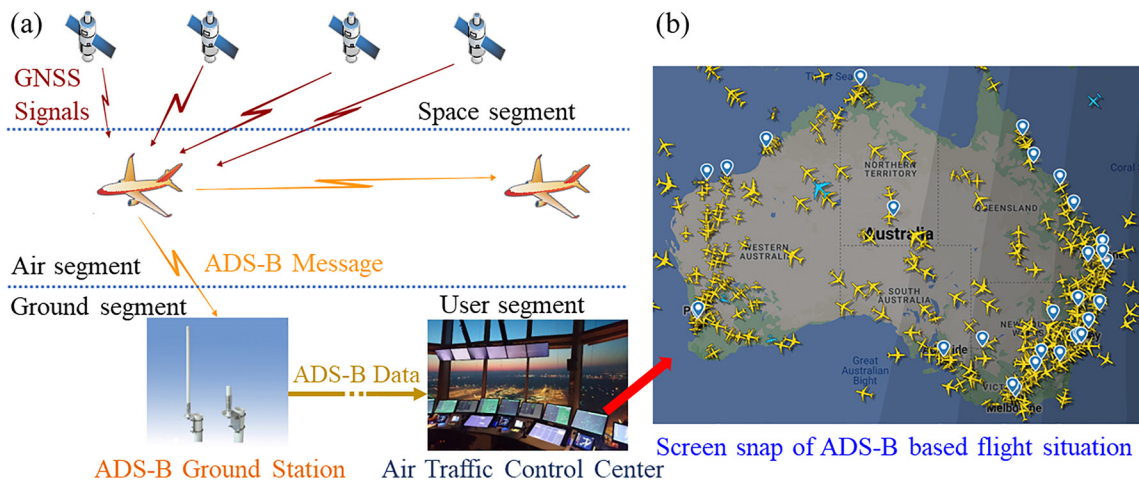


**Figure 6.** Schematic diagram of the Automatic Dependent Surveillance-Broadcast (ADS-B)-based air traffic management system. (a) The working principle of ADS-B. (b) The screen snap of the ADS-B-based flight situation.

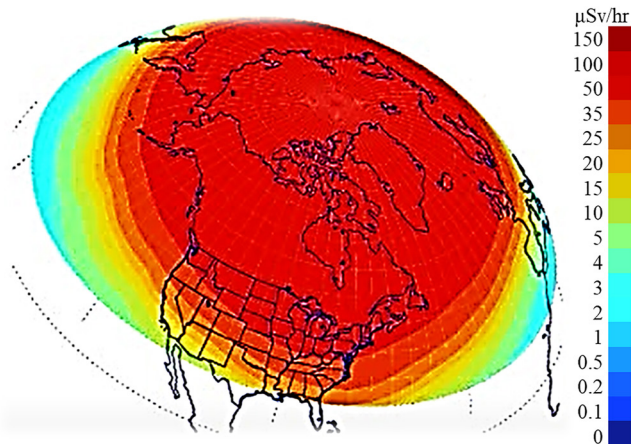


**Figure 7.** Effective dose (galactic cosmic radiation and solar energetic particles) at the altitude of 11 km at UT = 12:00 on 28 October 2003. The data source is based on the Nowcast of Aerospace Ionizing Radiation System via <http://sol.spacenvironment.net/~nairas/Gallery.html>.

We assume that the airlines will choose to cancel the flight if  $R_i$  is above a critical limit. Flight cancellation is one of the most conservative but reliable measures (Jiao et al., 2013). To the best of our knowledge, there are still no international regulations on cosmic radiation limits for a certain flight plan. Therefore, it is up to each airline's responsibility to assess the radiation threat and take appropriate actions accordingly (Xue, Yang, Liu, et al., 2022). For example, an international flight (callsign: CPA829) took off from the Toronto Pearson International Airport (43.68°N, 79.63°W) at 05:53 UTC and landed at the Hong Kong International Airport (23.31°N, 113.91°E) at 20:57 UTC. The estimated aviation radiation doses were 128 μSv on 27 October, 499 μSv on 28 October, 448 μSv on 29 October, and 263 μSv on 30 October. If the cosmic radiation limit is 100 μSv, CPA829 would have to be canceled in these 4 days. If the cosmic radiation limit is changed to 500 μSv, CPA829 could operate as usual in these 4 days. If the cosmic radiation limit is set as 400 μSv, CPA829 would be canceled on 28 and 29 October. Figure 8 shows the number of flight cancellations and corresponding costs based on the values in Table 2, for different cosmic radiation limits ranging from 100 to 1,000 μSv. Obviously, there were more flight cancellations on 28–29 October 2003 than that on other days, which could be explained by the elevated cosmic radiation during these 2 days. For detailed information, please refer Movie S1. NCRP (2013) mandates that the monthly radiation during pregnancy cannot exceed 500 μSv. If we set the cosmic radiation limit to 500 μSv, the cancellation costs would be €30.06 million on 28 October 2003, €18.56 million on 29 October 2003, and €0.35 million on 30 October 2003. In contrast, if the limit is set to 1,000 μSv, the total flight cancellation cost would be reduced to €2.77 million.

Apart from canceling flights, airlines can also reroute flights and lower flight altitudes to reduce the extremely high aviation radiation exposure (Saito et al., 2021). Rerouting is not considered in this study due to the possibility of increased fuel consumption and possible airspace rights infringement. Lowering flight altitudes seems efficient to reduce aviation exposure due to the atmosphere protection. Herein, we assume that flights at an altitude of 9 km or below would have minimum cosmic radiation. Therefore, flights can avoid exceeding the cosmic radiation

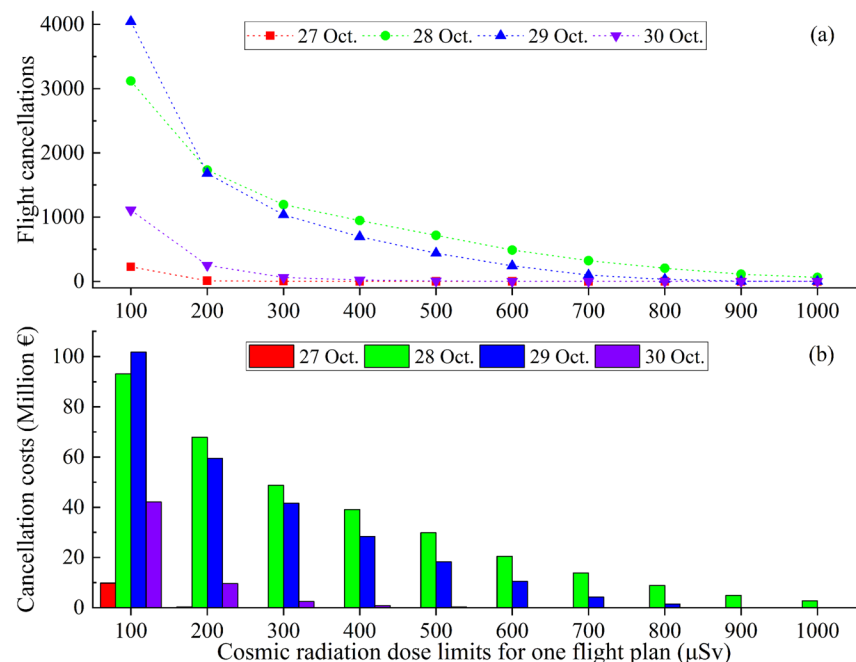


**Figure 8.** The number of canceled flights (a) and the corresponding cancellation costs (b) under different cosmic radiation dose limits.

threshold by lowering the flight altitude to 9 km. According to Appendix A, the additional fuel costs caused by lowering flight altitudes would be €5.24 million on 28 October 2003, €3.15 million on 29 October 2003, and €0.07 million on 30 October 2003. It seems that lowering flight altitudes is a much better choice because the expenses are remarkably less than canceling flights. However, airspace capacity in each flight level needs to be considered during real-world operations, as it may cause air traffic congestion and flight safety problem.

## 6. Conclusions and Discussions

Space weather effects are a multidisciplinary issue that can fundamentally impact a wide range of technologies and operations in space and on Earth. However, its economic implications on flight operation remain quite uncertain and cost estimates are wildly divergent due to the lack of consensus on the realistic technical footprint of severe space weather events. This study aims to evaluate the economic costs of space weather on aviation from the perspective of air traffic management, assuming that an extreme solar storm similar in strength to the 2003 Halloween storm occurred in April 2019. The flight cancellation costs caused by communication blackout range from €0.21 million to €2.20 million per day. Besides, the flight cancellation costs caused by elevated aviation radiation exposure (€2.77 million to €48.97 million) account for the majority of the total economic costs. In contrast, the total costs caused by GNSS navigation failure are €2.43 million during the space weather event because aircraft can use ground navigation method as a backup. Besides, additional flight delay costs and increased air traffic controller workload cannot be ignored although this study does not have a deep investigation into this area. The worst space weather events in the future and their impacts on GNSS applications are unknown yet. Therefore, improving the forecast of solar storm effects will help reduce the corresponding economic costs and improve flight safety. For example, if the durations of HF communication blackouts can be correctly forecasted, airlines can adjust flight schedules instead of canceling polar flights unnecessarily, which can considerably reduce cancellation costs. Cosmic radiation forecasts can also significantly impact airline decisions. Due to the Forbush effect, the neutron monitoring count rates on 29 October 2003 were 22% lower than the initial background level (Meier & Matthiä, 2014). If ICAO global space weather centers can provide airlines with this reduced value of cosmic radiation, unnecessary flight cancellations can be avoided.

The economic losses due to space weather are compared with the losses of two extreme cases. The direct demand losses of air transportation services induced by the terrorist attack on 11 September 2001 ranged from \$214.3 billion to \$420.5 billion (Gordon et al., 2007). The 2010 Eyjafjallajökull eruption in Iceland resulted in the closure of over 300 European airports during 15–21 April 2010, which caused an economic loss of 1.7–3.3 billion Euros (Alexander, 2013; Mazzocchi et al., 2010). In the 2001 and 2010 extreme cases, a large number of airports were completely closed, and all flights were canceled. They were different from the space weather case in which only a relatively small portion of flights were affected. Compared to these two appalling events, we have to acknowledge that the 2003 Halloween storm would have relatively small economic effects on aviation. That can be explained by the fundamental properties of space weather effects on aviation and the resilience of the air traffic management system. The effects include high-frequency communication blackouts, GNSS-based navigation and surveillance failure, and massive cosmic radiation. However, aviation communications rely primarily on VHF (only HF communications in the polar region); aircraft navigation can be accomplished using ground navigation aids, which cover the majority of terminal maneuvering areas; radar systems have always been used for real-time surveillance; the majority of cosmic radiation can be shielded by the Earth's atmosphere and magnetic field, and only a few dozens of flights at high latitudes may be affected. Furthermore, in this study, we did not account for the flight delay costs associated with airports and airlines, as flight cancellations are prevalent in conditions involving HF communication blackouts for polar flights and substantial aviation radiation exposure for flights in high latitudes. The required aircraft separation distances based on satellite navigation are smaller than those based on ground navigation. Due to the switch from satellite navigation to ground navigation, the required aircraft separation distances in the airspace will be enlarged. This will inevitably cause traffic delays to schedule all the flights with a smaller density in the airspace. Regarding the potential economic costs of satellite navigation failure on future air traffic in 2030, please refer to (Xue, Yang, & Liu, 2022), which quantifies flight delay costs including airborne delay cost and ground delay cost.

The space weather event selected in this study is the Halloween solar storm of 2003, which may occur once each solar cycle (11 years). If a 1-in-100-year solar storm (e.g., 1859 Carrington event) occurs in the future, the economic effects on air traffic will likely be much more significant. During such an event, the majority of

satellites, such as navigation satellites and communication satellites, may be inoperable, and widespread power outages may emerge (Eastwood et al., 2017; Ritter et al., 2020). As a result, from the perspective of air traffic management, the number of flight cancellations will likely be substantially greater than those in this study and they are requested to remain on the ground until all systems recover. This is of great interest for future study. It is worth mentioning that our methodology can also be useful for estimating the economic costs of weak and moderate space weather events, as a routine assessment of air traffic.

## Appendix A: Aircraft Capacity and Fuel Burn Information

The nominal fuel consumption in different Flight Levels (1 FL = 100 ft) according to the Base of Aircraft Data (BADA) (EUROCONTROL, 2022).

Aircraft types	Capacity seats	Fuel burn (kg/min)	
		291 FL	361 FL
B773	380	125.4	118.7
B789	195	97.7	88
A333	290	108.7	87.75
B772	360	115.3	104.35
A350	350	119.4	102.8
B788	240	92.9	82.55
B744	420	179.4	155.9
A388	520	240.8	213.1
B763	260	89.1	77.3
A332	250	110.7	91.75

## Data Availability Statement

The Dst values were obtained from OmniWeb (<https://omniweb.gsfc.nasa.gov/form/dx1.html>). The TEC data were obtained from IGS (<https://cddis.nasa.gov/archive/gnss/products/ionex/>). The cosmic radiation rate data were obtained from the Nowcast of Aerospace Ionizing Radiation System (NAIRS) (<http://sol.spacenvironment.net/~nairs/Gallery.html>). The GNSS data were obtained from IGS (<https://cddis.nasa.gov/archive/gnss/data/daily/>). The flight data can be obtained from Opensky (<https://opensky-network.org>).

## References

- Alexander, D. (2013). Volcanic ash in the atmosphere and risks for civil aviation: A study in European crisis management. *International Journal of Disaster Risk Science*, 4(1), 9–19. <https://doi.org/10.1007/s13753-013-0003-0>
- Bagshaw, M. (2008). Cosmic radiation in commercial aviation. *Travel Medicine and Infectious Disease*, 6(3), 125–127. <https://doi.org/10.1016/j.tmaid.2007.10.003>
- Bolduc, L. (2002). GIC observations and studies in the Hydro-Québec power system. *Journal of Atmospheric and Solar-Terrestrial Physics*, 64(16), 1793–1802. [https://doi.org/10.1016/S1364-6826\(02\)00128-1](https://doi.org/10.1016/S1364-6826(02)00128-1)
- Cameron, T., Fiori, R., Themens, D., Warrington, E., Thayaparan, T., & Galeschuk, D. (2022). Evaluation of the effect of sporadic-E on high frequency radio wave propagation in the Arctic. *Journal of Atmospheric and Solar-Terrestrial Physics*, 228, 105826. <https://doi.org/10.1016/j.jastp.2022.105826>
- Cannon, P., Angling, M., Barclay, L., Curry, C., Dyer, C., Edwards, R., et al. (2013). *Extreme space weather: Impacts on engineered systems and infrastructure*. Royal Academy of Engineering. Retrieved from <https://eprints.lancs.ac.uk/id/eprint/64443>
- Cao, Y., Jin, L., Nguyen, N. V., Landry, S., Sun, D., & Post, J. (2014). Evaluation of fuel benefits depending on continuous descent approach procedures. *Air Traffic Control Quarterly*, 22(3), 251–275. <https://doi.org/10.2514/atcq.22.3.251>
- Chen, B., & Liu, Z. (2015). A comprehensive evaluation and analysis of the performance of multiple tropospheric models in China region. *IEEE Transactions on Geoscience and Remote Sensing*, 54(2), 663–678. <https://doi.org/10.1109/TGRS.2015.2456099>
- Delta (2010). Space weather and Delta's polar routes. Retrieved from <https://www.swpc.noaa.gov/sites/default/files/images/u33/HEITZMAN%20SWW%202010.pdf>
- Doherty, P., Coster, A. J., & Murtagh, W. (2004). Space weather effects of October–November 2003. *GPS Solutions*, 8(4), 267–271. <https://doi.org/10.1007/s10291-004-0109-3>

## Acknowledgments

This work was supported by the Hong Kong Research Grants Council (RGC) projects (B-Q84W RGC/Gov No. PolyU 15205821), the Emerging Frontier Area (EFA) Scheme of Research Institute for Sustainable Urban Development (RISUD) of the Hong Kong Polytechnic University under Grant 1-BBWJ, the Stable Support Plan Program of Shenzhen Natural Science Fund (Grant 20200925153644003), and Shenzhen Science and Technology Program (Grant JCYJ20220530113402004). The project support (ZVVC-ZVN6) from the Hong Kong Polytechnic University is also appreciated. We thank WASAVIES team for providing the radiation dose rates.



- Eastwood, J., Biffis, E., Hapgood, M., Green, L., Bisi, M., Bentley, R., et al. (2017). The economic impact of space weather: Where do we stand? *Risk Analysis*, 37(2), 206–218. <https://doi.org/10.1111/risa.12765>
- Eastwood, J., Hapgood, M., Biffis, E., Benedetti, D., Bisi, M., Green, L., et al. (2018). Quantifying the economic value of space weather forecasting for power grids: An exploratory study. *Space Weather*, 16(12), 2052–2067. <https://doi.org/10.1029/2018SW002003>
- Enge, P., Enge, N., Walter, T., & Eldredge, L. (2015). Aviation benefits from satellite navigation. *New Space*, 3(1), 19–35. <https://doi.org/10.1089/space.2014.0011>
- Eroshenko, E., Belov, A., Boteler, D., Gaidash, S., Lobkov, S., Pirjola, R., & Trichtchenko, L. (2010). Effects of strong geomagnetic storms on Northern railways in Russia. *Advances in Space Research*, 46(9), 1102–1110. <https://doi.org/10.1016/j.asr.2010.05.017>
- EUROCONTROL. (2020). Standard inputs for economic analyses. Supporting European Aviation. Retrieved from <https://www.eurocontrol.int/publication/eurocontrol-standard-inputs-economic-analyses>
- EUROCONTROL. (2022). User manual for the Base of Aircraft Data (BADA) revision 3.16. Retrieved from <https://www.eurocontrol.int/model/bada>
- Gonzalez, W. D., Tsurutani, B. T., & Clúa de Gonzalez, A. L. (1999). Interplanetary origin of geomagnetic storms. *Space Science Reviews*, 88(3), 529–562. <https://doi.org/10.1023/A:1005160129098>
- Gopalswamy, N., Yashiro, S., Liu, Y., Michalek, G., Vourlidis, A., Kaiser, M., & Howard, R. (2005). Coronal mass ejections and other extreme characteristics of the 2003 October–November solar eruptions. *Journal of Geophysical Research*, 110(A9), 2005. <https://doi.org/10.1029/2004JA010958>
- Gordon, P., Moore, J. E., Park, J. Y., & Richardson, H. W. (2007). The economic impacts of a terrorist attack on the US commercial aviation system. *Risk Analysis: An International Journal*, 27(3), 505–512. <https://doi.org/10.1111/j.1539-6924.2007.00903.x>
- Guo, J., & Geng, J. (2018). GPS satellite clock determination in case of inter-frequency clock biases for triple-frequency precise point positioning. *Journal of Geodesy*, 92(10), 1133–1142. <https://doi.org/10.1007/s00190-017-1106-y>
- Humphreys, T. E., Psiaki, M. L., & Kintner, P. M. (2010). Modeling the effects of ionospheric scintillation on GPS carrier phase tracking. *IEEE Transactions on Aerospace and Electronic Systems*, 46(4), 1624–1637. <https://doi.org/10.1109/TAES.2010.5595583>
- IATA. (2022). Jet fuel price monitor. International Air Transport Association. Retrieved from <https://www.iata.org/en/publications/economics/fuel-monitor/>
- ICAO. (2008). *Manual on air traffic management system requirements*. International Civil Aviation Organization. Retrieved from <https://www.icao.int/airnavigation/IMP/Documents/Doc%209882%20Manual%20on%20ATM%20Requirements.pdf>
- ICAO. (2016). Procedures for Air Navigation and Air Traffic Management Pans-atm Doc 4444. Retrieved from <https://ops.group/blog/wp-content/uploads/2017/03/ICAO-Doc4444-Pans-Atm-16thEdition-2016-OPSGROUP.pdf>
- ICAO. (2018). *ICAO Annex 10 Volume 1 Radio Navigation Aids*. International Civil Aviation Organization. Retrieved from <https://ffac.ch/wp-content/uploads/2020/09/ICAO-Annex-10-Aeronautical-Telecommunications-Vol-I-Radio-Navigation-Aids.pdf>
- ICRP. (2016). Radiological protection from cosmic radiation in aviation. In *Annals of the ICRP*. Retrieved from <https://www.icrp.org/publication.asp?id=ICRP%20Publication%20132>
- Jheng, S.-L., Jan, S.-S., Chen, Y.-H., & Lo, S. (2020). 1090 MHz ADS-B based wide area multilateration system for alternative positioning navigation and timing. *IEEE Sensors Journal*, 20(16), 9490–9501. <https://doi.org/10.1109/JSEN.2020.2988514>
- Jiao, Y., Morton, Y. T., Taylor, S., & Pelgrum, W. (2013). Characterization of high-latitude ionospheric scintillation of GPS signals. *Radio Science*, 48(6), 698–708. <https://doi.org/10.1002/2013RS005259>
- Kauristie, K., Andries, J., Beck, P., Berdermann, J., Berghmans, D., Cesaroni, C., et al. (2021). Space weather services for civil aviation—Challenges and solutions. *Remote Sensing*, 13(18), 3685. <https://doi.org/10.3390/rs13183685>
- Kelly, M. A., Comberiate, J. M., Miller, E. S., & Paxton, L. J. (2014). Progress toward forecasting of space weather effects on UHF SATCOM after Operation Anaconda. *Space Weather*, 12(10), 601–611. <https://doi.org/10.1002/2014SW001081>
- Kim, J., Kim, Y., Song, J., Kim, D., Park, M., & Kee, C. (2019). Performance improvement of time-differenced carrier phase measurement-based integrated GPS/INS considering noise correlation. *Sensors*, 19(14), 3084. <https://doi.org/10.3390/s19143084>
- Langley, R. B., Teunissen, P. J., & Montenbruck, O. (2017). Introduction to GNSS. In *Springer handbook of global navigation satellite systems* (pp. 3–23). Springer. <https://doi.org/10.1007/978-3-319-42928-1>
- Li, H. (2021). Sino-Russian center for space weather monitoring operational. Retrieved from [https://english.www.gov.cn/news/international-exchanges/20211118/content\\_WS6195ae24c6d0df57f98e5205.html](https://english.www.gov.cn/news/international-exchanges/20211118/content_WS6195ae24c6d0df57f98e5205.html)
- Loto'aniu, T., Singer, H., Rodríguez, J., Green, J., Denig, W., Biesecker, D., & Angelopoulos, V. (2015). Space weather conditions during the Galaxy 15 spacecraft anomaly. *Space Weather*, 13(8), 484–502. <https://doi.org/10.1002/2015SW001239>
- Marqué, C., Klein, K.-L., Monstein, C., Opgenoorth, H., Pulkkinen, A., Buchert, S., et al. (2018). Solar radio emission as a disturbance of aeronautical radionavigation. *Journal of Space Weather and Space Climate*, 8, A42. <https://doi.org/10.1051/swsc/2018029>
- Maynard, T., Smith, N., & Gonzalez, S. (2013). Solar storm risk to the North American electric grid. *Lloyd's*, 11. <https://assets.lloyds.com/assets/pdf-solar-storm-risk-to-the-north-american-electric-grid/1/pdf-Solar-Storm-Risk-to-the-North-American-Electric-Grid.pdf>
- Mazzocchi, M., Hansstein, F., & Ragona, M. (2010). The 2010 volcanic ash cloud and its financial impact on the European airline industry. In *Proceedings of CESifo forum* (pp. 92–100). Retrieved from <https://www.econstor.eu/bitstream/10419/166397/1/cesifo-forum-v11-y2010-i2-p092-100.pdf>
- Meier, M. M., & Matthäi, D. (2014). A space weather index for the radiation field at aviation altitudes. *Journal of Space Weather and Space Climate*, 4, A13. <https://doi.org/10.1051/swsc/2014010>
- Mertens, C. J., Meier, M. M., Brown, S., Norman, R. B., & Xu, X. (2013). NAIRAS aircraft radiation model development, dose climatology, and initial validation. *Space Weather*, 11(10), 603–635. <https://doi.org/10.1002/swe.20100>
- NASA. (2017). *Space radiation is risky business for the human body*. National Aeronautics and Space Administration. Retrieved from <https://www.nasa.gov/feature/space-radiation-is-risky-business-for-the-human-body>
- National Research Council. (2008). Severe space weather events: Understanding societal and economic impacts: A workshop report. [https://books.google.com.hk/books?hl=zh-CN&lr=&id=\\_nadAgAAQBAJ&oi=fnd&pg=PR1&dq=Severe+space+weather+events:+Understanding+societal+and+economic+impacts:+A+workshop+report&ots=54dWTqVoBY&sig=aypHXkSUASnGFXRDhAyU1NzuE-&redir\\_esc=y#v=onepage&q=Severe%20space%20weather%20events%3A%20Understanding%20societal%20and%20economic%20impacts%3A%20A%20workshop%20report&f=false](https://books.google.com.hk/books?hl=zh-CN&lr=&id=_nadAgAAQBAJ&oi=fnd&pg=PR1&dq=Severe+space+weather+events:+Understanding+societal+and+economic+impacts:+A+workshop+report&ots=54dWTqVoBY&sig=aypHXkSUASnGFXRDhAyU1NzuE-&redir_esc=y#v=onepage&q=Severe%20space%20weather%20events%3A%20Understanding%20societal%20and%20economic%20impacts%3A%20A%20workshop%20report&f=false)
- NCRP. (2013). Preconception and prenatal radiation exposure: Health effects and protective guidance. Retrieved from <https://www.apfa.org/wp-content/uploads/2017/12/preconception-and-prenatal-radiation-exposure.pdf>
- Neal, J. J., Rodger, C. J., & Green, J. C. (2013). Empirical determination of solar proton access to the atmosphere: Impact on polar flight paths. *Space Weather*, 11(7), 420–433. <https://doi.org/10.1002/swe.20066>
- NOAA. (2004). Intense space weather storms October 19–November 07, 2003. Retrieved from <https://repository.library.noaa.gov/view/noaa/6995>



- Odenwald, S., Green, J., & Taylor, W. (2006). Forecasting the impact of an 1859-calibre superstorm on satellite resources. *Advances in Space Research*, 38(2), 280–297. <https://doi.org/10.1016/j.asr.2005.10.046>
- Oughton, E., Copic, J., Skelton, A., Kesaite, V., Yeo, Z., Ruffle, S., & Ralph, D. (2016). *Helios solar storm scenario: Cambridge risk framework series, Centre for risk studies*. University of Cambridge. Retrieved from <https://www.jbs.cam.ac.uk/wp-content/uploads/2020/08/aig-helios-solar-storm-16-june.pdf>
- Oughton, E. J., Hapgood, M., Richardson, G. S., Beggan, C. D., Thomson, A. W., Gibbs, M., et al. (2019). A risk assessment framework for the socioeconomic impacts of electricity transmission infrastructure failure due to space weather: An application to the United Kingdom. *Risk Analysis*, 39(5), 1022–1043. <https://doi.org/10.1111/risa.13229>
- Oughton, E. J., Skelton, A., Horne, R. B., Thomson, A. W., & Gaunt, C. T. (2017). Quantifying the daily economic impact of extreme space weather due to failure in electricity transmission infrastructure. *Space Weather*, 15(1), 65–83. <https://doi.org/10.1002/2016SW001491>
- Ricke, K., Drouet, L., Caldeira, K., & Tavoni, M. (2018). Country-level social cost of carbon. *Nature Climate Change*, 8(10), 895–900. <https://doi.org/10.1038/s41558-018-0282-y>
- Ritter, S., Rotko, D., Halpin, S., Nawal, A., Farias, A., Patel, K., et al. (2020). International legal and ethical issues of a future carrington event: Existing frameworks, shortcomings, and recommendations. *New Space*, 8(1), 23–30. <https://doi.org/10.1089/space.2019.0026>
- Rutledge, R., & Desbios, S. (2018). Space weather focus: Impacts of a severe space weather event on aviation operations. In *World Meteorological Organization Commission for Aeronautical Meteorology (CAeM) Newsletter 1*.
- Ryan, J. M., Lockwood, J. A., & Debrunner, H. (2000). Solar energetic particles. *Space Science Reviews*, 93(1), 35–53. <https://doi.org/10.1023/A:1026580008909>
- Saito, S., Wickramasinghe, N. K., Sato, T., & Shiota, D. (2021). Estimate of economic impact of atmospheric radiation storm associated with solar energetic particle events on aircraft operations. *Earth Planets and Space*, 73(1), 1–10. <https://doi.org/10.1186/s40623-021-01377-5>
- Sauer, H. H., & Wilkinson, D. C. (2008). Global mapping of ionospheric HF/VHF radio wave absorption due to solar energetic protons. *Space Weather*, 6(12), S12002. <https://doi.org/10.1029/2008SW000399>
- Schnell, M., Epplé, U., Shutin, D., & Schneckenburger, N. (2014). Ldacs: Future aeronautical communications for air-traffic management. *IEEE Communications Magazine*, 52(5), 104–110. <https://doi.org/10.1109/MCOM.2014.6815900>
- Schulte in den Bäumen, H., Moran, D., Lenzen, M., Cairns, I., & Steenge, A. (2014). How severe space weather can disrupt global supply chains. *Natural Hazards and Earth System Sciences*, 14(10), 2749–2759. <https://doi.org/10.5194/nhess-14-2749-2014>
- Sparks, L., Altshuler, E., Pandya, N., Blanch, J., & Walter, T. (2022). WAAS and the ionosphere—A historical perspective: Monitoring storms. *NAVIGATION. Journal of the Institute of Navigation*, 69(1), navi.503. <https://doi.org/10.33012/navi.503>
- Sun, R., Hsu, L.-T., Xue, D., Zhang, G., & Ochieng, W. Y. (2019). GPS signal reception classification using adaptive neuro-fuzzy inference system. *Journal of Navigation*, 72(3), 685–701. <https://doi.org/10.1017/S0373463318000899>
- Svestka, Z. (2012). *Solar flares* (Vol. 8). Springer Science & Business Media. Retrieved from [https://books.google.com.hk/books?hl=zh-CN&lr=&id=AtnsCAAQBAJ&oi=fnd&pg=PP12&dq=Solar+flares&ots=fDtFAZjrgv&sig=iW6NcnkzHdaJammW6G\\_vcRAxEf4&redir\\_esc=y#v=onepage&q=Solar%20flares&f=false](https://books.google.com.hk/books?hl=zh-CN&lr=&id=AtnsCAAQBAJ&oi=fnd&pg=PP12&dq=Solar+flares&ots=fDtFAZjrgv&sig=iW6NcnkzHdaJammW6G_vcRAxEf4&redir_esc=y#v=onepage&q=Solar%20flares&f=false)
- Tuo, F., Zhou, L., Xu, C., Yao, Y., Ren, T., & Zhou, Q. (2012). Measurement of cosmic radiation dose to air crew connecting for a typical polar route flight. *Journal of Radioanalytical and Nuclear Chemistry*, 293(3), 935–939. <https://doi.org/10.1007/s10967-012-1775-1>
- Viljanen, A., Pulkkinen, A., Pirjola, R., Pajunpää, K., Posio, P., & Koistinen, A. (2006). Recordings of geomagnetically induced currents and a nowcasting service of the Finnish natural gas pipeline system. *Space Weather*, 4(10), S10004. <https://doi.org/10.1029/2006SW000234>
- Watari, S. (2015). Estimation of geomagnetically induced currents based on the measurement data of a transformer in a Japanese power network and geoelectric field observations. *Earth Planets and Space*, 67(1), 1–12. <https://doi.org/10.1186/s40623-015-0253-8>
- Webb, D. F., & Howard, T. A. (2012). Coronal mass ejections: Observations. *Living Reviews in Solar Physics*, 9(1), 1–83. <https://doi.org/10.12942/lrsp-2012-3>
- Wen, X., Chung, S.-H., Ji, P., & Sheu, J.-B. (2022). Individual scheduling approach for multi-class airline cabin crew with manpower requirement heterogeneity. *Transportation Research Part E: Logistics and Transportation Review*, 163, 102763. <https://doi.org/10.1016/j.tre.2022.102763>
- Xue, D., Hsu, L.-T., Wu, C.-L., Lee, C.-H., & Ng, K. K. (2021). Cooperative surveillance systems and digital-technology enabler for a real-time standard terminal arrival schedule displacement. *Advanced Engineering Informatics*, 50, 101402. <https://doi.org/10.1016/j.aei.2021.101402>
- Xue, D., Liu, Z., Wang, B., & Yang, J. (2021). Impacts of COVID-19 on aircraft usage and fuel consumption: A case study on four Chinese international airports. *Journal of Air Transport Management*, 95, 102106. <https://doi.org/10.1016/j.jairtraman.2021.102106>
- Xue, D., Yang, J., & Liu, Z. (2022). Potential impact of GNSS positioning errors on the satellite-navigation-based air traffic management. *Space Weather*, 20(7), e2022SW003144. <https://doi.org/10.1029/2022SW003144>
- Xue, D., Yang, J., Liu, Z., & Wang, B. (2022). An optimized solution to long-distance flight routes under extreme cosmic radiation. *Space Weather*, 20(12), e2022SW003264. <https://doi.org/10.1029/2022SW003264>
- Yamashiki, Y. A., Fujita, M., Sato, T., Maehara, H., Notsu, Y., & Shibata, K. (2020). Cost estimation for alternative aviation plans against potential radiation exposure associated with solar proton events for the airline industry. *Evolutionary and Institutional Economics Review*, 17(2), 487–499. <https://doi.org/10.1007/s40844-020-00163-4>
- Yang, Z., Zhang, Q., Ding, X., & Chen, W. (2020). Analysis of the quality of daily DEM generation with geosynchronous InSAR. *Engineering*, 6(8), 913–918. <https://doi.org/10.1016/j.eng.2020.07.003>
- Yang, Z.-Y., & Sheu, R.-J. (2020). An in-depth analysis of aviation route doses for the longest distance flight from Taiwan. *Radiation Physics and Chemistry*, 168, 108548. <https://doi.org/10.1016/j.radphyschem.2019.108548>
- Yu, S., & Liu, Z. (2021). The ionospheric condition and GPS positioning performance during the 2013 tropical cyclone Usagi event in the Hong Kong region. *Earth Planets and Space*, 73(1), 1–16. <https://doi.org/10.1186/s40623-021-01388-2>
- Zhang, S., Du, S., Li, W., & Wang, G. (2019). Evaluation of the GPS precise orbit and clock corrections from MADOCA real-time products. *Sensors*, 19(11), 2580. <https://doi.org/10.3390/s19112580>